ZIP9 is a Druggable Determinant of Sex Differences in Melanoma

Cristina Aguirre-Portolés[1], Riley Payne[2], Aspen Trautz[1], J. Kevin Foskett[2], Christopher A. Natale[1], John T. Seykora[1], Todd W. Ridky[1]*

[1]Department of Dermatology, Perelman School of Medicine, University of Pennsylvania.

[2]Department of Physiology, Perelman School of Medicine, University of Pennsylvania, Philadelphia, PA. USA.

Running Title: ZIP9 promotes melanoma in males.

Key words: Skin cancer, melanoma, sex disparities in cancer, steroids, testosterone, ZIP9.

Financial support: T.W.R. is supported by grant from the NIH/NCI (R01 CA163566, R41CA228695), and by the Stiefel award from the Dermatology Foundation. This work was also supported in part by the Penn Skin Biology and Diseases Resource-based Center (P30-AR069589), the Melanoma Research Foundation and DOD to T.W.R., and R37 GM56328 to J.K.F.

***Corresponding author:** Todd W. Ridky. Department of Dermatology, Perelman School of Medicine, University of Pennsylvania. BRB1010. 421 Curie Blvd. Philadelphia, PA 19104. ridky@pennmedicine.upenn.edu.

18 **Abstract**

19 Melanoma and most other cancers occur more frequently, and have worse prognosis, in males
20 compared with females. Though sex steroids are thought to be involved, classical androgen and
21 estrogen receptors are not detectable in most melanomas. Here we show that testosterone
22 promotes melanoma proliferation by activating ZIP9 (*SLC39A9*), a zinc transporter that is not
23 intentionally targeted by available therapeutics, but is widely expressed in human melanoma.
24 This testosterone activity requires zinc influx, MAPK activation and YAP1 nuclear translocation.
25 We demonstrate that FDA approved inhibitors of the classical androgen receptor also inhibit
26 ZIP9, and thereby antagonize the pro-tumorigenic effects of testosterone in melanoma. In male
27 mice, androgen receptor inhibitors suppressed growth of ZIP9-expressing melanomas, but had no
28 effect on isogenic melanomas lacking ZIP9, nor on melanomas in females. These data suggest
29 that ZIP9 might be effectively targeted in melanoma and other cancers by repurposing androgen
30 receptor inhibitors that are currently approved only for prostate cancer.

31

32 **Significance**

33 Melanoma outcomes are worse in males than in females. Some of this difference is driven by
34 testosterone signaling through ZIP9, a nonclassical testosterone receptor. Drugs that target AR
35 can be repurposed to block ZIP9, and inhibit melanoma in males.

36 **Introduction**

37 Cancer incidence and mortality are higher in males than in females in the U.S. and worldwide[1,2].
38 In the U.S., males are 15% more likely to develop cancer, and 40% more likely to die from this
39 disease than females[1]. These sex differences were recognized as early as 1949[3], are observed in
40 the majority of cancer types from non-reproductive tissues[1], and remain even after controlling for
41 known risk factors such as environmental and occupational exposures[4]. While recent advances in
42 modern targeted and immune therapeutics have markedly improved survival for both female and
43 male melanoma patients[5], females still have more favorable outcomes[1,4]. Defining the
44 mechanisms underlying the broad and persistent sex differences in cancer incidence and
45 outcomes will address a major unresolved question in cancer pathobiology.

46 We previously showed that the female sex hormone estradiol inhibits melanoma
47 proliferation and tumor growth *in vivo*. This effect is independent of biologic sex of the tumor,
48 independent of classical estrogen receptors (ER), and results from activation of a nonclassical
49 surface estrogen receptor on melanocytes and melanoma cells called the G Protein Estrogen
50 Receptor (GPER)[6,7]. This work led us to consider whether male sex hormone signaling might
51 also contribute to female vs. male differences in melanoma progression.

52 Testosterone is the most abundant androgen and circulates at much higher levels in
53 males (630 ng/dl) than in females (32 ng/dl)[8]. In males, higher levels of circulating testosterone
54 also correlate with increased melanoma incidence[9]. Testosterone promotes proliferation *in vitro*
55 in non-gonadal cell types including adipocytes[10], mouse skeletal muscle myoblasts[11],
56 glioblastoma-derived cells[12], lung cancer cell lines[13] and melanoma[14]. As the classical androgen
57 receptor (AR) is not consistently detected in most of these tissues, the receptor(s) mediating the
58 testosterone-dependent increased proliferation and the corresponding downstream mechanisms

59 are not yet defined. Also unknown is whether this androgen activity observed *in vitro* is relevant
60 to cancer progression *in vivo*.

61 Here we studied 98 human melanocytic lesions (nevus, primary and metastatic melanoma
62 from both males and females) and did not detect AR in any of them. However, in nearly all
63 samples, we readily detected ZIP9, a membrane localized zinc transporter recently discovered in
64 Atlantic Croaker (fish) cells to be a activated by testosterone[15].

65 Here, we use genetic and pharmacologic approaches to target ZIP9 in multiple melanoma
66 models *in vitro* and *in vivo*. These functional studies define a previously unappreciated
67 nonclassical testosterone signaling pathway through ZIP9, establish a novel mechanistic link
68 between male androgens and melanoma pathobiology, and highlight a potential new therapeutic
69 opportunity by repurposing currently available drugs.

70

71 **Materials and Methods**

72

73 **Cell culture and proliferation assays**

74 YUMM1.7, SH-4 and SK-MEL-2 cells were purchased from ATCC (YUMM1.7 ATCC® CRL-
75 3362™; SH-4 ATCC® CRL-7724™; SK-MEL-2 ATCC® HTB-68™) and cultured in DMEM
76 (Mediatech, Manassas, VA, USA) with 5% FBS (Invitrogen, Carlsbad, CA, USA) and 1%
77 Penicillin-Streptomycin (Thermo Fisher Scientific. #15140122). SK-MEL-3 cells were
78 purchased from ATCC (ATCC® HTB-69™ and cultured in McCoy's 5A (Modified) Medium
79 with 10% FBS (Invitrogen, Carlsbad, CA, USA) and 1% Penicillin-Streptomycin. SK-MEL-24
80 cells were purchased from ATCC (ATCC® HTB-71™) and cultured in Eagle's Minimum
81 Essential Medium with 15% FBS and 1% Penicillin-Streptomycin. WM46 melanoma cells were
82 a gift from Meenhard Herlyn (Wistar Institute, Philadelphia, PA, USA) and were cultured in

83 TU2% media. Tumor cells were regularly tested using MycoAlert Mycoplasma Detection Kit
84 from Lonza (Allendale, NJ, USA). Early passage cells were used after obtaining them directly
85 from ATCC. For monitoring cell proliferation $10x10^5$ YUMM1.7 or $12x10^5$ WM46 cells were
86 seed per well in 12-well Cell culture Plates. All the experiments performed in this work utilized
87 charcoal stripped serum (Fetal Bovine Serum, charcoal stripped, USDA-approved regions, One
88 Shot™ format. Catalogue number #A3382101; Thermofisher Scientific). Cells were treated
89 every second day and manually counted in triplicate using a hemocytometer (Testosterone
90 solution and Testosterone-CMO-BSA were purchased from Sigma-Aldrich, T5411-1ML and
91 T3392-10MG respectively). All the experiments were performed in cell populations that were in
92 culture during a maximum of 3 weeks (5 passages in average) since thaw from the corresponding
93 stock.
94
95 **CRISPR-Cas9 mediated ablation of Slc39A9**
96 We used lentiviral transduction to deliver dox-inducible Cas9 and gRNA targeting exon 1 of
97 Slc39A9 in human WM46 and murine YUMM1.7 melanoma cells. Transduced cells were
98 selected with puromycin, and single cells subsequently isolated, expanded and examined for
99 ZIP9 protein expression, compared to clones isolated in parallel with no doxycycline treatment.
100 The following gRNA sequences were used (5'-3'):
101 hZIP9_gRNA_Fw caccgTTGGTGGGATGTTACGTGGC
102 hZIP9_gRNA_Rv aaacGCCACGTAACATCCCACCAAC
103 hZIP9_gRNA_Fw caccgCGTGGCCGGAATCATTCC
104 hZIP9_gRNA_Rv aaacGGAATGATTCCGGCCACG

105 To map the targeted sequencing, the region surrounding the gRNA target sequence was
106 amplified in both WM46 (282bp) and YUMM1.7 (259bp) isogenic clones. The following
107 primers were used (5'-3'): hZIP9_CRISPRmut_Fw:
108 TAAGCAGAATTCATGGATGATTTCATCTCC
109 hZIP9_CRISPRmut_Rv:TAAGTAAGTCCAAGCTTCTGCTGCTTTGTCTGATGCA.
110 mZIP9_CRISPRmut_F:TAAGCAGAATTCATGGATGACTTTCTCTC.
111 mZIP9_CRISPRmut_Rv TAAGTAAGTCCAAGCTTGATATTTCTGCTGCTTTGT.
112 Once amplified, DNA fragments were cloned into pUC19 vector using EcoRI and HindDIII
113 sites, and sequenced (Sanger) by the DNA Sequencing Facility (University of Pennsylvania).
114 Sequences were analyzed using the free software CRISP-ID (V1.1) and ICE Analysis by
115 Synthego were the knock-out scores were obtained.
116
117 **Zinc influx analysis**
118 WM46 cells were loaded with 5 µM FluoZin™-3, AM cell permeant™ (Thermo Fisher
119 Scientific, #F24195), for 20 minutes then incubated in 2 Ca Tyrode's solution (in mM: 140
120 NaCl, 5 KCl, 1 $MgCl_2$, 2 $CaCl_2$, 10 glucose and 5 (Na) Pyruvate – pH 7.4) for 5-10 minutes at
121 room temperature prior to imaging. Cells were imaged on a Nikon Ti microscope using a
122 20x/0.75 NA objective for fluorescence at 340 nm and 380nm excitation/515 nm emission (Ca^{2+}-
123 free Fura2 or FluoZin™-3) and 380 nm excitation/515 nm emission (Ca^{2+}-free Fura2 FluoZin™-
124 3). Coverslips were perfused at 1-3 mL/min following this protocol: Ca^{2+} Tyrode's (0-30 secs);
125 Ca^{2+} Tyrode's + DMSO & 5 uM Zinc (30-90 secs); Ca^{2+} Tyrode's + Testosterone & 5µM Zinc
126 (90-360 secs); Ca^{2+} Tyrode's + Testosterone + BIC & 5 uM Zn (360-470 secs); Ca^{2+} Tyrode's
127 washout (470-500 secs). 100 milliseconds exposure images for each wavelength were collected

128 every 2 seconds. For analyzing the long-term consequences of testosterone treatment, cells were
129 treated with the androgen for 96 hours and then loaded FluoZin™-3. Cells were incubated with
130 FluoZin™-3 following manufacturer recommendation and exposed to 400nM Zn pyrithione or
131 $ZnCl_2$. Images were acquired with EVOS BLA. Fluorescence was quantitated using ImageJ
132 (National Institutes of Health, Bethesda, MD, USA), and statistical analyses were performed
133 using Graphpad Prism software.
134
135 **Reverse Phase Protein Array (RPPA)**
136 We used the Functional Proteomics Core at MD Anderson
137 (https://www.mdanderson.org/research/research-resources/core-facilities/functional-proteomics-
138 rppa-core.html) to perform a 447-element Reverse Phase Protein Array (RPPA) analysis of
139 human melanoma cells grown in medium with stripped serum and treated with testosterone
140 (100nM) for 0, 30', 60' and 8 hours. Cells were tripsinized and washed with PBS. After
141 centrifugation (5 minutes; 1200rpm), supernatant was discarded, and cells were frozen at -80ºC
142 prior to be sent to the Functional Proteomics Core at MD Anderson.
143
144 **Western blot, immunofluorescence and antibodies**
145 Adherent cells were washed once with PBS and lysed with 8M urea containing 50mM NaCl and
146 50mM Tris-HCl, pH 8.3, 10mM dithiothreitol, 50mM iodoacetamide. Lysates were quantified
147 (Bradford assay), normalized, reduced, and resolved by SDS gel electrophoresis on 4–15%
148 Tris/Glycine gels (Bio-Rad, Hercules, CA, USA). Resolved protein was transferred to PVDF
149 membranes (Millipore, Billerica, MA, USA) using a Semi-Dry Transfer Cell (Bio-Rad), blocked
150 in 5% BSA in TBS-T and probed with primary antibodies recognizing β-actin (Cell Signaling

151 Technology, #3700. Mouse. Lot:14 1:4000, Danvers, MA, USA), ZIP9 (Abcam, #137205,
152 Rabbit mAb. Lot: GR3231323-8. 1:500), P-ERK (Cell Signaling Technology, Phospho-p44/42
153 MAPK (Erk1/2) (Thr202/Tyr204) (D13.14.4E) XP® Rabbit mAb #4370. Lot. 24 1:1000), ERK
154 (Cell Signaling Technology, p44/42 MAPK (Erk1/2) (137F5) Rabbit mAb. Lot: 28 #4695,
155 1:1000), Androgen Receptor [(D6F11) XP® Rabbit mAb #5153. Lot: 7], Recombinant Anti-
156 Androgen Receptor antibody [EPR1535(2)] (ab133273. Antibody already validated by the
157 Human Protein Atlas), RSK1/RSK2/RSK3 [(32D7) Rabbit mAb #9355. Lot:3], Phospho-
158 p90RSK [(Thr359/Ser363)Antibody #9344. Lot: 15]. After incubation with the appropriate
159 secondary antibody [(Rabbit Anti-Mouse IgG H&L (Biotin) preabsoFS9rbed (ab7074); Anti-
160 mouse IgG, HRP-linked Antibody #7076. 1:2000)] proteins were detected using ClarityTM
161 Western ECL Substrate (Bio-Rad. #170-5060). All western blots were repeated at least 3 times.
162 To monitor YAP1 nuclear translocation by western blot analysis, nuclear fractionation was
163 performed using protein lysis buffer containing 10mM HEPES, 1mM KCl, 1.5mM MgCl2 and
164 10% glycerol (Buffer A). After washing the adherent cells with DPBS, samples were
165 resuspended in Buffer A and incubated for 5 minutes on ice in the presence of 0.1% Triton-X-
166 100. After centrifugation, the nuclear fraction remained as a pellet while the supernatant
167 corresponding to the cytosolic fraction. Nuclear fraction was washed with Buffer A. After
168 centrifugation, the nuclear fraction was resuspended in RIPA buffer and samples were boiled for
169 5 min prior to sample loading. The cytosolic fraction was centrifuged for 15 min at 13500 rpm.
170 Only the supernatant was kept after centrifugation. Western blot was performed as described
171 before and the following antibodies were used for protein detection: β-tubulin (Cell Signaling
172 Technology, β-Tubulin (9F3) Rabbit mAb #2128. 1:1000), PARP (Cell Signaling Technology,
173 Rabbit mAb #9542. 1:1000), YAP1 (Cell Signaling Technology, YAP (D8H1X) XP® Rabbit

174 mAb #14074. 1:1000). For immunofluorescence in adherent cells, samples were fixed with 4%
175 paraformaldehyde (Affymetrix; #19943) for 7 min at room temperature and permeabilized with
176 iced-cold methanol. After blocking with 10% FBS:0.03%Triton-X100, primary antibodies were
177 incubated overnight in blocking solution (β-actin and YAP1 antibodies detailed above). After
178 three washes in DPBS:0.03% Triton X-100) cells were incubated with secondary antibodies for
179 45 minutes at room temperature [(Goat anti-Mouse IgG (H+L) Highly Cross-Adsorbed
180 Secondary Antibody, Alexa Fluor 594. Goat anti-Rabbit IgG (H+L) Highly Cross-Adsorbed
181 Secondary Antibody, Alexa Fluor 488)]. Cells were rinsed with PBS-0.03%-Triton three times
182 and coverslips were mounted with ProLong Gold antifade reagent with DAPI (#P36935; Thermo
183 Fisher Scientific). Images were captured using a Leica DM IL microscope and registered using
184 LAS software. For fluorescence intensity quantification ImageJ software (National Institutes of
185 Health, Bethesda, MD, USA) was used, and statistical analyses were performed with GraphPad
186 Prism software.
187
188 **Immunohistochemistry and quantification**
189 FFPE tissue microarrays (ME1004h: Malignant melanoma, metastatic malignant melanoma and
190 nevus tissue array) were obtained from US Biomax, Inc. (Derwood, MD). For the staining with
191 anti-ZIP9 antibody [(SLC39A9 Antibody (PA5-52485), Thermofisher Scientific, Waltham,
192 MA)], slides were deparaffinized and rehydrated following the standard immunohistochemistry
193 protocol [(xylenes 5 minutes x 3, 100% alcohol (5 min. x 3), 95% alcohol (5 min.), 80% alcohol
194 (5 min.), 70% alcohol (5 min.), and 50% alcohol (5 min.) and finished with distilled water)]. The
195 antigen retrieval was done by loading the slides into a retriever (Electron Microscopy Sciences
196 EMS) with R-Buffer A. After 20 minutes, samples were allowed to cool for 30 minutes inside

197 the retriever and for 20 minutes at room temperature. Samples were washed twice with PBS and
198 blocked with Dako Dual Endogenous Enzyme Block (Code S2003. Agilent Santa Clara, CA) for
199 20 minutes at R.T. Samples were washed twice with PBS and blocked for 20 minutes with 2
200 drops of Vector Avidin Block. After washing twice with PBS, slides were blocked for 20
201 minutes with two drops of Vector Biotin Block (Avidin/Biotin Blocking kit. SP-2001. Vector
202 Laboratories, Inc. Burlingame, CA). Samples were washed twice with PBS with Protein Block
203 Serum-Free Ready-To-Use for 30 minutes at R.T. (Code X0909. Agilent Santa Clara, CA).
204 Primary antibody was prepared 1:500 in PBST (100µl per slide) and samples were incubated
205 overnight at 4°C. Samples were washed three times with PBS and incubated with Biotinylated
206 Secondary antibody (Vectastain Kit, Peroxidase Rabbit IgG, PK-4001) for one hour at R.T. After
207 three washes with PBS, ABC reagent (prepared 30 minutes in advance) was added and samples
208 were incubated for 30 minutes at R.T. Samples were washed twice with PBS and incubated for 3
209 minutes with ImmPACT® DAB Substrate, Peroxidase (HRP) (SK-4105. Vector laboratories,
210 Burlingame, CA). Tissues were counterstained with hematoxylin (30 seconds, R.T.) (GHS316.
211 Sigma-Aldrich) dehydrated, and mounted with SecureMount (Fisher HealthCare™
212 PROTOCOL™ Mounting Media. #022-208. Fisher Scientific. Thermofisher Scientific). John T.
213 Seykora M.D., Ph.D, performed scoring of the stained tissue microarray, and scoring index was
214 determined by scoring the percentage of positive cells on a scale of 0 to 3 as well as the intensity
215 of ZIP9 staining on a scale of 0 to 4 (1=1-25%, 2=26-50%, 3=51-75%, 4=76-100%).

216 The staining of the tissue microarrays (ME1004h) for AR detection was performed by
217 University of Pennsylvania Pathology Clinical Service Center—Anatomic Pathology Division,
218 using the highest grade, CLIA (Clinical Laboratory Improvement Amendments) certified and
219 validated test available. Briefly, five-micron sections of formalin-fixed paraffin-embedded tissue

220 were stained using antibody against Androgen Receptor [(Leica AR-318-L-CE, clone AR27
221 (clone AR27, 1:25)]. Staining was done on a Leica Bond-IIITM instrument using the Bond
222 Polymer Refine Detection System (Leica Microsystems DS9800). Heat-induced epitope retrieval
223 was done for 20 minutes with ER2 solution (Leica Microsystems AR9640). All the experiment
224 was done at room temperature. Slides are washed three times between each step with bond wash
225 buffer or water. The slides were reviewed and scored in blinded fashion by a board-certified U.
226 Penn pathologist. Prostate tissue was used as the positive control.
227
228 **Immunocytochemistry**
229 To detect ZIP9 protein in WM46 isogenic clones, the protocol described in ProSciΨ™ for
230 immunocytochemistry. Briefly, cells were fixed in 4% PFA for 7 minutes. After two washes with
231 PBS (5min), cells were permeabilized with PBS/0.1% Triton X-100 for 1 minute at R.T. Cells
232 were washed twice with PBS on a shaker. Once treated with 1.5% H_2O_2/PBS solution for 15
233 minutes (R.T.), cells were washed again and blocked with 5%BSA for one hour at R.T. For
234 primary antibody incubation, α-ZIP9 antibody [(SLC39A9 Antibody (PA5-52485),
235 Thermofisher Scientific, Waltham, MA)] was diluted 1:500 in 1% BSA and cells were incubated
236 overnight at 4ºC. After washing three times with PBS on a shaker, the slide was incubated with
237 Biotinylated Secondary antibody (Vectastain Kit, Peroxidase Rabbit IgG, PK-4001) for one hour
238 at R.T. Cells were washed three times with PBS, ABC reagent (prepared 30 minutes in advance)
239 was added and samples were incubated for 30 minutes at R.T. After three washes with PBS,
240 samples were incubated for 1.5 minutes with Vector Laboratories DAB Peroxidase (HRP)
241 Substrate Kit (NC9276270. Vector laboratories, Burlingame, CA). Cells were counterstain with
242 hematoxylin (10 seconds, R.T.) (GHS316. Sigma-Aldrich) and mounted with SecureMount

243 (Fisher HealthCare™ PROTOCOL™ Mounting Media. #022-208. Fisher Scientific.
244 Thermofisher Scientific).
245
246 **Cell membrane labeling with testosterone-BSA-FITC**
247 WM46 were seeded over coverslips in p12-well culture plate, after 24 hours cells TU2% media
248 was removed, and cells were grown in Serum-free TU media for 24 hours. Cells were treated
249 with APA (8mM) or DMSO as vehicle control. After one hour, cells were treated with 0.25µM
250 testosterone 3-(O-carboxymethyl) oxime:BSA-fluorescein isothiocyanate (T-BSA-FITC)
251 conjugate (T5771, Sigma-Aldrich, Munich, Germany) diluted in Tris-Buffer (pH 7.2) for 20 min
252 at room temperature. Negative control cells were incubated with 0.25 µM BSA-FITC (A9771,
253 Sigma-Aldrich, Munich, Germany) diluted in Tris-Buffer (pH 7.2) for 20 min at room
254 temperature. The medium was then aspirated, and cells were fixed for 7 minutes with 4%PFA.
255 Cells were washed three times with PBS (5 minutes each) and mounted with ProLong Gold
256 antifade reagent with DAPI (#P36935; Thermo Fisher Scientific). Images were captured using a
257 Leica DM IL microscope and registered using LAS software.
258
259 **Quantitative RT-PCR**
260 RNA was extracted using RNeasy kit (Qiagen. #74104) following the manufacturer's
261 instructions. cDNA was obtained using High Capacity cDNA Reverse Transcription Kit
262 (Applied Biosystems #4368814). For quantitative real-time PCR, PowerUP™ SYBR™ Green
263 Master Mix (Applied Biosystems #A25741) was used. ViiA 7 Real-Time PCR System was used
264 to perform the reaction (Applied Biosystems). Values were corrected by β-actin expression. The

265 $2^{-\Delta\Delta Ct}$ method was applied to calculate the relative gene expression. Primers used for the
266 amplification are included in Table S2.
267
268 **Mice, subcutaneous tumors and pharmacologic treatments**
269 All mice were purchased from Taconic Biosciences, Inc. (Rensselaer, NY, USA). 8- to 10-week
270 old male and female C57BL/6NTac or IcrTac:ICR-Prkdcscid mice were allowed to reach
271 sexually mature ages or to acclimatize for one week prior to being used in experiments. These
272 studies were performed without inclusion/exclusion criteria or blinding but included
273 randomization. Based on a two-fold anticipated effect, we performed experiments with at least 5
274 biological replicates. All procedures were performed in accordance with International Animal
275 Care and Use Committee (IACUC)-approved protocols at the University of Pennsylvania.
276 Subcutaneous tumors were initiated by injecting tumor cells in 50% Matrigel (Corning, Bedford,
277 MA, USA) into the subcutaneous space on the right flanks of mice. 10×10^6 human WM46 or 10
278 x 10^5 murine YUMM1.7 cells were used for each tumor. Oral administration of vehicle,
279 bicalutamide (30mg/kg/day) or apalutamide (20mg/kg/day) was performed daily. 100µl of drug
280 was administrated by oral gavage [10%DMSO:90%Vehicle (15% ethanol:85% sesame oil)].
281 Each experiment include n=5 replicates, which provide 100% power to detect at least a 50%
282 difference between groups with 95% confidence. The size of each animal cohort was determined
283 by estimating biologically relevant effect sizes between control and treated groups and then
284 using the minimum number of animals that could reveal statistical significance using the
285 indicated tests of significance. When in vivo experiments were performed with female, mice
286 located in different cages, animals were randomized prior to cell inoculation or drug treatment.
287 All animals housed within the same cage were placed within the same treatment group. Weight

288 and health status of the mice as well as tumor growth were monitored daily. As subcutaneous
289 tumors grew in mice, perpendicular tumor diameters were measured using calipers. Volume was
290 calculated using the formula $L \times W^2 \times 0.52$, where L is the longest dimension and W is the
291 perpendicular dimension. Animals were euthanized when tumors exceeded a protocol-specified
292 size of 15 mm in the longest dimension. Secondary endpoints include severe ulceration, death,
293 and any other condition that falls within the IACUC guidelines for Rodent Tumor and Cancer
294 Models at the University of Pennsylvania.
295
296 **Statistical analysis**
297 For experiments comparing two groups (treated vs control), significance was calculated using the
298 Mann-Whitney test. For experiments with more than two groups, one-way ANOVA with
299 Tukey's honest significance difference test was performed. For the tumor growth studies *in vivo*,
300 non-linear regression analysis was performed to get the Exponential Growth Equation and
301 doubling times for tumor growth. To analyze the slopes of the curves and to compare them
302 between groups, linear regression analysis was performed. All the statistical analyses in this
303 work were performed using Graphpad Prism Software. Error bars represent standard error of the
304 mean (SEM). **** p value≤0.0001; *** p value≤0.001; ** p value≤0.01; * p value≤0.05;
305 n.s>0.05.
306
307 **<u>Results</u>**
308
309 **Melanoma tumors grow more quickly in male vs. female mice**.
310
311 To test whether preclinical melanoma models recapitulate the male vs. female survival disparity
312 observed in humans, we first determined growth of human BRAF-driven melanoma (WM46,

313 female origin, BRaf^{V600E}; CDK4^{R24C}). Tumors grew faster in immunodeficient SCID male mice
314 compared with matched female mice (Fig. 1A and Fig. S1A), indicating that the differences do
315 not depend on T and/or B cell immune responses. To test whether this phenotype extends to a
316 genetically-engineered preclinical mouse model, we used murine YUMM1.7 cells (male origin,
317 BRaf$^{V600E/wt}$;Pten$^{-/-}$CdkN2a$^{-/-}$)[16] in syngeneic immunocompetent C57BL/6 mice. These tumors
318 also consistently grew faster in male mice compared with matched females (Fig. S1B).
319

320 **Testosterone, but not dihydrotestosterone, promotes proliferation in melanoma cells**
321 **independent of the classical androgen receptor.**

322 Physiologic concentrations of testosterone promoted proliferation of both normal early passage
323 primary human melanocytes and melanoma cells (Fig. 1B, C and Fig. S1C). The proliferative
324 response to testosterone correlated with dose and was saturable, suggesting a specific receptor-
325 mediated activity. In contrast, dihydrotestosterone (DHT) had no effect on proliferation of these
326 cell types across a wide concentration range (Fig. 1C). Dihydrotestosterone is a more potent AR
327 agonist than testosterone[17,18]. The fact that the melanocytes and melanoma cells responded to
328 testosterone, but not to DHT (Fig. 1B, 1C, Fig. S1C, S1D and S1E), suggests the possibility that
329 testosterone effects in these cells are mediated by the nonclassical androgen receptor ZIP9, as
330 ZIP9 has a much higher affinity for testosterone than for dihydroteststerone[15]. Further suggesting
331 the idea that a nonclassical androgen receptor mediates these observed testosterone effects, we
332 were unable to detect AR protein (via western blotting using 2 different AR antibodies, or via
333 immunofluorescence) in primary melanocytes, or in any of the 8 melanoma cell lines we have
334 tested (Table S1). We did, however, readily detect AR protein in 2 prostate cancer lines used as
335 positive controls (Fig. 1D and Fig. S1F and S1G). Consistent with this lack of detectable AR

336 protein, AR transcript was not detected via RNASeq in any of 6 different primary human
337 melanocyte cultures. In contrast, *SLC39A9*/ZIP9 transcript, as well as transcript for the classical
338 nuclear glucocorticoid receptor *NR3C1*, and for the melanocyte marker *MC1R*, were each readily
339 detected in all the cell lines (Fig. 1E).

340 To test whether testosterone effects in melanoma cells are mediated by a surface receptor,
341 we next treated WM46 and SK-MEL-24 human melanoma cells, (female and male derived,
342 respectively) with a membrane-impermeable testosterone analogue [(Testosterone 3-(O-
343 carboxymethyl)oxime: BSA] that is incapable of activating AR (AR is necessarily active in the
344 nucleus). This compound and free testosterone each similarly promoted melanoma proliferation
345 (Fig. S2A), supporting the idea that a non-classical androgen receptor located in the cellular
346 membrane was responsible for the observed phenotype.

347 ZIP9 is broadly expressed in most cancers (Fig. S2B), normal human melanocytes, and
348 all melanoma lines that we tested (Fig. 2A). ZIP9 transports zinc (Zn^{++}) across cell and organelle
349 membranes into the cytoplasm and is the only steroid receptor known to directly regulate zinc
350 homeostasis[19]. To test whether testosterone activates this ZIP9 activity in melanoma, we used the
351 fluorescent Zn^{++}-specific probe FluoZin-3. Testosterone induced a rapid increase in cytosolic
352 free Zn^{++} ($[Zn^{++}]_i$) in human melanoma cells (Fig. 2B), that was followed by a sustained
353 elevation for at least 2 days in the presence of testosterone (Fig. 2C). We determined that Zn^{++}
354 influx was necessary for the testosterone-dependent increase in melanoma cell proliferation, as
355 treatment with the Zn^{++} chelator N,N,N′,N′-tetrakis (2-pyridinylmethyl)-1,2-ethanediamine
356 (TPEN), blocked testosterone induced proliferation at TPEN concentrations that had no
357 significant effect on proliferation when used alone (Fig. 2D and Fig. S2C).

358 Although TPEN has high affinity for Zn^{++}, it also has some ability to chelate copper[20]. To
359 test whether copper flux might contribute to testosterone effects on melanoma proliferation, we
360 treated WM46 cells with $CuSO_4$, which had no significant effect on cell proliferation (Fig. S2D).
361 Moreover, the highly specific copper chelator bathocuproinedisulfonic acid (BCS), did not affect
362 the proliferative response to testosterone, nor did BCS affect testosterone induced Zn^{++} influx
363 (Fig. S2E and Fig. S2F).

364 After determining that Zn^{++} influx was necessary for testosterone-induced proliferation,
365 we next tested whether increased Zn^{++} was sufficient to increase melanoma proliferation.
366 Exogenous zinc pyrithione (also a Zn^{++} ionophore), and $ZnCl_2$ each increased melanoma
367 proliferation (Fig. 2E). Other biologically-relevant divalent cations, Fe^{++} and Mn^{++}, known to be
368 transported by other ZIP family members[21], had no effect on proliferation (Fig. 2E). Together,
369 these results demonstrate that testosterone, but not DHT, promotes zinc dependent proliferation
370 in melanoma cells that express ZIP9 and lack detectable AR.

371 We next used immunocytochemistry to test whether AR and/or ZIP9 protein are
372 expressed in human melanocytic lesions (14 benign nevi, 63 primary melanomas, and 21
373 metastatic melanomas from both males and females). AR was determined in tissue sections using
374 a highly validated CLIA (Clinical Laboratory Improvement Amendments) certified method in
375 the clinical pathology lab at the Hospital of the University of Pennsylvania. This procedure uses
376 a validated antibody different from the two we used for western blotting and
377 immunofluorescence. Each tissue was scored in a blinded fashion by a board-certified
378 pathologist. While AR was readily detectable in prostate tissue used as positive control, AR was
379 not detected in any of the nevi, nor in the melanomas (Fig. 2F). In parallel, we analyzed the same
380 samples for ZIP9. CLIA grade ZIP9 IHC is not available. However, we validated our ZIP9

381 antibody using parental WM46 ZIP9 positive (wtZIP9) and isogenic ZIP9 negative (ΔZIP9) cell
382 lines. These cells were grown on chamber slides and processed for IHC in parallel with the
383 human samples. The antibody used labeled only the wtZIP9 cells. ZIP9 protein was observed in
384 100% of the nevi, 97% of primary melanomas and 100% of the metastatic samples (Fig. 2G).
385 Further, the ZIP9 relative staining intensity positively correlated with tumor stage (Fig. 2H).
386 ZIP9 intensity was skewed toward higher intensity scores (Score 2 and 3) in metastatic tumors
387 (Score 0: 0%; Score 1: 46.6%; Score 2: 40%; Score 3: 13.3% of tumors) vs. primary tumors
388 (Score 0: 1.72%; Score 1: 60.34%; Score 2: 29.31%; Score 3: 8.62% of tumors. None of the nevi
389 showed the highest level (Score 3) observed in the melanomas. No significant differences in
390 ZIP9 staining were observed between males and females (Fig. S2G). Similarly, no correlation
391 was observed between ZIP9 expression and the age of the patient (Fig. S2H).

392 ZIP9 is broadly expressed and its pro-melanoma activity is likely limited more by the
393 availability of testosterone, than by ZIP9 itself. However, we did question whether ZIP9
394 expression correlates with clinical melanoma outcomes in people. We used *OSskm*[22] to analyze
395 pooled data from 1085 tumors (563 death events) from multiple studies (GSE17275, GSE19234,
396 GSE22155_GPL6102, GSE22155_GPL6947, GSE50509, GSE46517, GSE53118, GSE65904,
397 GSE98394 and TCGA. Although not significant (p-value=0.11), there is a trend associating
398 higher ZIP9 expression with shorter survival (HR=1.2039) (Fig S3A and Table S2), consistent
399 with the idea that ZIP9 promotes melanoma progression. Importantly, when patients are stratified
400 by sex (TCGA), the trend between high ZIP9 expression and poor survival is observed in males
401 (H.R.=1.27, C.I. 95% 0.64-2.52), but not in females (H.R. 1.01, C.I. 95% 0.41-2.46) (Fig. S3B).
402 No correlation was found between ZIP9 expression and several other prognostic melanoma
403 markers including age, tumor ulceration, Clark level, mitotic rate, and aneuploidy Fig. S3C).

404 **Testosterone signaling through ZIP9 promotes melanoma growth**

405 To determine whether ZIP9 mediates testosterone effects, we used CRISPR-Cas9 and gRNA
406 targeting Slc39A9 exon 1 to ablate ZIP9 in human (WM46) melanoma and in murine
407 (YUMM1.7) melanoma. Isogenic clonal populations of parental ZIP9-expressing (wtZIP9) and
408 ZIP9-ablated (ΔZIP9) cells were established, and the mutations disrupting the reading frame
409 were mapped by sequencing (Fig. S4A, S4B and S4C). ZIP9 protein was not detectable in ΔZIP9
410 cells (Fig. 2F, Fig. 3A, Fig. 3B and Fig. S4D). ΔZIP9 cells did not respond to testosterone,
411 whereas isogenic wtZIP9 control clones responded similarly to the parental wild-type cells (Fig.
412 3A, 3B and Fig. S4E).

413 The testosterone insensitive phenotype associated with CRISPR-Cas9 engineered ZIP9 loss
414 was rescued by expression of a human ZIP9 transgene. Lentiviral mediated constitutive ZIP9
415 expression in the ΔZIP9 WM46 cells restored both ZIP9 protein and the proliferative response to
416 testosterone, verifying the on-target effects of the CRISPR-Cas9 mediated ZIP9 ablation (Fig.
417 S4F, S4G).

418 Consistent with the conclusion that ZIP9 is the major mediator of testosterone effects in
419 these melanoma cells, exposure to testosterone failed to increase $[Zn^{++}]_i$ in ΔZIP9 cells (Fig. 3C
420 and 3D). Intracellular free zinc levels following exogenous zinc exposure are similar between
421 wtZIP9 and ΔZIP9 cells (Fig. S4H), indicating that while other zinc transporters are expressed in
422 human melanoma cells, ZIP9 induces a rapid, ZIP9-dependent, increase in $[Zn^{++}]_i$ that is required
423 for the increased proliferation in melanoma cells (Fig. 3D and Fig. S4H).

424

425

426 **Testosterone-induced melanoma proliferation through ZIP9 requires downstream MAPK**
427 **and YAP1 activation**

428 Although the studies detailed above show that testosterone promotes melanoma proliferation via
429 ZIP9 dependent Zn^{++} influx, zinc is involved in myriad cellular processes, making it difficult to
430 predict *a priori* which downstream signaling pathways are required for the testosterone activity.
431 To start identifying these, we used a 447-element Reverse Phase Protein Array (RPPA) analysis
432 of human WM46 melanoma cells treated with testosterone for 0, 30, 60 and 480 min. While the
433 relative expression of most represented proteins was unaffected by testosterone, some were
434 significantly under or overexpressed, including several with known tumor-promoting or tumor-
435 suppressive functions (Fig. 4A and Table S3). Downregulated proteins included 14-3-3ε, a tumor
436 suppressor and negative YAP1 regulator previously implicated in liver, lung, and gastric
437 cancers[23], and CDKN2A (p16), a cyclin-dependent kinase (CDK) inhibitor, and one of the most
438 studied tumor suppressors[24]. Upregulated proteins included key elements of tumor-promoting
439 pathways, most notably phosphorylated ERK (T202; Y204) and YAP1 (Fig. 4A).
440 Importantly, ΔZIP9 cells displayed decreased basal levels of ERK phosphorylation compared
441 with isogenic wild-type clones (Fig. S5A). MAPK activation was necessary for the testosterone-
442 dependent proliferative response, as the specific ATP-competitive ERK1/2 inhibitor, ulixertinib[25]
443 (RVD-523; Ei) blocked the testosterone-dependent proliferative response, at ulixertinib
444 concentrations that had no effect on the basal proliferation rate when used alone (Fig. 4B).
445 Testosterone-dependent ZIP9 activation appeared to render WM46 cells more sensitive to
446 ulixertinib, as cell viability was compromised when they were treated with both testosterone and
447 RVD-523. This vulnerability to combination treatment seems to be specific and ZIP9 dependent,

448 as ΔZIP9 cells treated with both testosterone and ulixertinib proliferated at rates comparable to
449 controls (Fig. 4B).

450 We determined that YAP1 activation is also required for the augmented proliferative
451 response driven by testosterone. YAP1 is a transcriptional coactivator whose activity is largely
452 regulated by its localization[26]. Testosterone induced rapid YAP1 translocation from cytoplasm to
453 nucleus in human melanoma cells in a ZIP9-dependent manner (Fig. 4C, 4D and Fig. S5B).
454 YAP1 subcellular localization is controlled largely by LATS, which phosphorylates YAP1 at
455 Serine 127 and thereby retains YAP1 in the cytoplasm[27]. The YAP1 inhibitor dobutamine also
456 promotes phosphorylation of YAP at Ser127[28]. Consistent with this, the testosterone induced
457 YAP1 nuclear localization and increase in cell proliferation were both blocked by dobutamine,
458 while this compound had no significant effect on its own (Fig. 4D, and Fig. 4E). When ZIP9
459 expression was rescued via lentiviral transduction of a ZIP9 transgene to ΔZIP9 WM46 cells,
460 testosterone dependent YAP1 translocation into the nucleus was also restored (Fig. S5C).

461 Testosterone promotion of YAP1 activity was evidenced by increased expression of
462 several well-known YAP1 target genes including CDC6, CTGF, CYR61 and THBS1. As
463 expected, these testosterone-induced expression changes were also blocked by dobutamine (Fig.
464 4F).

465

466 **Pharmacologic ZIP9 blockade inhibits testosterone-driven melanoma proliferation and**
467 **melanoma tumor growth *in vivo.***

468 We next tested whether FDA-approved drugs could be repurposed to effectively target
469 ZIP9. Although specific ZIP9 inhibitors are not yet developed, molecular modeling and
470 competition assays with fluorescent-tagged testosterone suggest that the androgen receptor

471 inhibitor bicalutamide (BIC) competes with testosterone for ZIP9 binding to the same
472 extracellular pocket and thereby acts as a competitive ZIP9 antagonist[29]. Bicalutamide was
473 developed and approved for prostate cancer and has now been largely replaced by enzalutamide
474 (ENZ) and apalutamide (APA), which are structurally related analogs with higher affinity for the
475 androgen receptor and greater clinical efficacy against advanced prostate cancer[30,31].

476 While ZIP9 was not known to be an androgen receptor at the time these drugs were
477 developed, we show here that they are nonetheless effective inhibitors of testosterone effects in
478 melanoma cells that express ZIP9, but that lack detectable AR. Each compound completely
479 blocked testosterone-induced proliferation and MAPK activation in several melanoma cell lines
480 (Fig. 5A, 5B). Importantly, these agents alone (without testosterone) had no effect on cell
481 proliferation (Fig. S6A). The testosterone dependent increase of intracellular zinc was also
482 efficiently blocked by bicalutamide (Fig. S6B). Moreover, ΔZIP9 cells transduced to re-express
483 ZIP9, responded to testosterone, and this effect was again blocked by bicalutamide (Fig. S6C).

484 To further confirm that these pharmacologic agents work through ZIP9, we next used
485 cyproterone acetate (CPA), an anti-androgen that blocks the testosterone interaction with AR, but
486 that does not bind to ZIP9[32]. In our melanoma cells, up to a 20-fold molar excess of CPA did not
487 significantly inhibit testosterone effects on proliferation, consistent with the conclusion that AR
488 is not the major mediator of testosterone effects in these melanoma models (Fig. S6D).
489 Importantly, response to testosterone and/or APA was independent on BRAF status, as SK-
490 MEL-2 cells (B-RAF^{wt}) responded well to testosterone, non-permeable testosterone, and to ZIP9
491 inhibition by apalutamide (Fig S6E).

492 BRAF inhibitors are useful in melanoma patients with BRAF driven tumors [33,34]. To test
493 whether combined targeted inhibition of BRAF and ZIP9 might be effective against BRAF

494 mutant melanoma we determined proliferation of human WM46 ($BRAF^{V600E}$) and murine
495 YUMM1.7 ($BRAF^{V600E}$) in the presence of the BRAF inhibitor PLX-4032 alone, and in
496 combination with apalutamide. Although addition of apalutamide to PLX-4032 was not
497 synergistic in WM46 cells (possibly because PLX-4032 alone was quite effective at limiting
498 proliferation), the combination of apalutamide and PLX-4032 was more effective in YUMM1.7
499 compared to either agent alone (Fig. S6F).

500 To test whether bicalutamide class AR inhibitors block the physical interaction between
501 testosterone and ZIP9 in melanoma, we performed direct binding assays using a membrane-
502 impermeable testosterone analogue (T-BSA-FITC). This reagent labels the plasma membrane
503 surface of wild-type ZIP9 expressing WM46 melanoma cells (Fig. 5C). This membrane bound
504 testosterone was displaced by apalutamide, demonstrating the specificity of the interaction (Fig.
505 5C). Further demonstrating that the binding is ZIP9 specific, testosterone localization at the
506 plasma membrane was markedly reduced in ΔZIP9 cells (Fig. 5C) that did not respond to
507 testosterone, nor to APA *in vitro* (Fig. 5D).

508 Next, we tested whether apalutamide and related analogs inhibit melanoma *in vivo*. For
509 this, we introduced wtZIP9 or isogenic ΔZIP9 human WM46 melanoma into SCID mice. Once-
510 daily systemically administered apalutamide (20 mg/kg/day via oral gavage) significantly
511 suppressed growth of wtZIP9 tumors in male mice and extended survival (doubling time for
512 tumor growth was 11.1 days for vehicle treated males and 25.2 days for APA treated males) (Fig.
513 5E, Fig. S7A). Similar results were obtained when males were treated with bicalutamide
514 (30mg/kg/day) (Fig. 5F). Importantly, bicalutamide had no effect on wtZIP9 tumors in female
515 mice, nor on ΔZIP9 tumors (Fig. 5F, G, Fig. S7B and C). Together, these data show that ZIP9
516 promotes melanoma progression specifically in males.

517 **Discussion**

518 High levels of circulating testosterone are associated with increased risk of early death
519 after a cancer diagnosis in men and women, and reaches 1.52 (1.20–1.91) (20.2-51.2 nmol/l) for
520 the highest quintile.[35] Together with this, other recent work correlating testosterone level with
521 the risk of 19 types of cancer [9] shows that higher free and total testosterone in men is associated
522 with higher risk of melanoma [free testosterone: 1.35 (95% CI 1.14, 1.61), total testosterone:
523 1.28 (95% CI 1.05, 1.55)] however, no association between testosterone and melanoma was
524 found in women [free testosterone: 0.96 (95% CI 0.77, 1.20), total testosterone: 0.95 (95% CI
525 0.82, 1.10)]. These epidemiological data support the idea that that testosterone promotes
526 melanoma. Outcomes for males are likely further worsened by the fact that they lack female
527 levels of estrogen, which is increasingly recognized to play protective roles against
528 melanoma[6,36,37].

529 Many have speculated how sex steroids contribute to sex differences in cancer
530 pathobiology, however, definitive functional studies are lacking, and the mechanisms by which
531 they contribute to the male-female cancer sex gap are only now emerging. The role of
532 nonclassical estrogen, progesterone, and testosterone receptors (GPER1, PAQR7, and ZIP9,
533 respectively) in cancer pathobiology has been largely unexplored. However, these are highly
534 likely to be significant contributors to sex specific pathobiology in melanoma (and other cancers)
535 as each are transcribed at much higher levels than the classical nuclear sex steroid receptors,
536 most of which are not detectable above background (Fig. S8A).

537 Circulating testosterone in humans generally ranges between 8-35nM[38]. We used 100 nM
538 in our *in vitro* experiments, a concentration used in diverse cell types in different labs [10,39,40]. For
539 biologically active small molecules including drugs, hormones, and ions, differences in IC_{50} and

540 saturating concentrations are often observed between *in vitro* and *in vivo* conditions. This results
541 from differences in compound stability and protein binding which affect half-life and the amount
542 of biologically available free vs. bound compound. These pharmacokinetic differences typically
543 make direct comparisons between *in vitro* and *in vivo* settings difficult. Many endogenous
544 ligands like testosterone, are only replenished in culture when the media is changed, whereas
545 homeostatic mechanisms keep testosterone levels stable *in vivo*. A higher starting concentration
546 *in vitro* may therefore be needed to maintain saturating levels for the entire time period between
547 media changes.

548 Testosterone promoted proliferation of melanoma cells in a saturable and dose-dependent
549 manner. Curiously, the same cell lines did not respond to DHT, which is generally considered
550 the more biologically active androgen. DHT displays 4-fold increased affinity than testosterone
551 for AR, and it dissociates from AR three time slower than testosterone[18]. Lack of response to
552 DHT in melanoma is consistent with the absence of detectable AR expression in the models used
553 for this study, and is highly consistent with our genetic data showing that ZIP9, which has higher
554 affinity for testosterone vs. DHT, is an important mediator of testosterone effects. Consistent
555 with this, a previous study in metastatic prostate cancer suggested that activation of the
556 migratory machinery depends solely in the activation of testosterone/ZIP9 pathway and not in
557 the interaction of this androgen with the nuclear AR[41].

558 We show here that ZIP9 activation, via testosterone binding, promotes an increase in
559 cytosolic zinc in melanoma cells. The mammalian family of zinc transporters SLC39A
560 comprises 14 members (ZIP1–14)[42] grouped into four subfamilies that were stablished according
561 to their amino acid sequence similarities. There may be roles for these other family members in
562 some cancers, as ZIP1 (SLC39A1, from ZIPII subfamily) has been associated with the regulation

563 of zinc uptake in prostate cancer cells[43]. However, the rapid increase of intracellular zinc through
564 ZIP1 appears to be AR dependent, as PC-3 cells only respond to testosterone after they are
565 transfected with exogenous AR. ZIP9 amino acid residues predicted to be most critical for
566 testosterone and bicalutamide binding include Ala167, Val241, Met248, and Ala167, Leu302,
567 Ser171, respectively[29], however only Ala167 is present in ZIP1, suggesting that this receptor
568 may not be similarly regulated by testosterone. Regarding other SLC39A proteins, sequence
569 analysis places ZIP9 as unique member of ZIPI subfamily[44], and it is the only one known to
570 interact with testosterone.

571 There may be many drivers of the cancer sex gap in humans, including differences in
572 immune surveillance[45]. However, differences in immune surveillance do not appear to be a major
573 driver of the differences in the melanoma models used for this study, as tumors progressed faster
574 not only in male vs. female syngeneic immunocompetent mice, but also in human melanomas
575 grown in male vs. female SCID mice. Therefore, the testosterone effects on melanoma in these
576 models are dependent on ZIP9, but independent of B and T cell mediated anti-tumor activity.
577 Consistent with this, ZIP9 expressing tumors responded to bicalutamide and apalutamide in
578 SCID mice.

579 As ZIP9 is widely expressed in nearly all tissues, it may be a major determinant of the sex
580 disparity in outcomes not just for melanoma, but also for many other cancer types. Consistent
581 with this, we observed that testosterone promotes proliferation of genetically diverse melanoma
582 lines and that this effect is blocked by bicalutamide (Fig. S9).

583 While this work clearly establishes a major role for ZIP9 in melanoma, we do recognize
584 the possibility that some melanoma cell lines, and perhaps even some human tumors, may
585 express a low level of AR that also impacts melanoma. However, any such tumor would still

586 likely also be affected by ZIP9. A recent report[46] also considered a possible role for testosterone
587 in melanoma and, consistent with our data, concluded that testosterone promotes melanoma
588 progression. Authors attributed this effect to the classical AR. However, that report did not
589 consider the nonclassical androgen receptor ZIP9. Critically, that study did not show that AR
590 was necessary for melanoma response to pharmacologic AR inhibitors, nor did it test whether
591 AR was a determinant of sex differences in melanoma.

592 The demonstration here that ZIP9 is pharmacologically accessible, suggests that ZIP9
593 may be a new eminently druggable therapeutic target (Fig. 6), and that currently approved
594 androgen receptor inhibitors might be useful in combination with current standard of care
595 therapeutics for a wide range of cancers, especially those that disproportionately affect males.

596

597 **Acknowledgements**

598 The authors thank the University of Pennsylvania Skin Biology and Disease Research-
599 based center for analysis of tissue sections and University of Pennsylvania Pathology Clinical
600 Service Center—Anatomic Pathology Division for the AR staining of the tissue microarray.

601

602 **References**

603 1. Siegel, R. L., Miller, K. D. & Jemal, A. Cancer statistics, 2020. *CA Cancer J Clin* **70**, 7–
604 30 (2020).
605 2. GLOBOCAN2018. https://bit.ly/2Vd3C6a.
606 3. Clemmesen, J. & Busk, T. Cancer Mortality Among Males and Females in Denmark,
607 England, and Switzerland: V. Incidence of Accessible and Inaccessible Cancers in Danish Towns
608 and Rural Areas. *Cancer Res* **9**, 415–421 (1949).
609 4. Hieken, T. J. *et al.* Sex-Based Differences in Melanoma Survival in a Contemporary
610 Patient Cohort. *Journal of Women's Health* (2020) doi:10.1089/jwh.2019.7851.
611 5. GLOBOCAN2018. Sex disparities in melanoma survival over time. shorturl.at/bkAI6.
612 6. Natale, C. A. *et al.* Activation of G protein-coupled estrogen receptor signaling inhibits
613 melanoma and improves response to immune checkpoint blockade. *Elife* **7**, (2018).
614 7. Natale, C. A. *et al.* Sex steroids regulate skin pigmentation through nonclassical

615 membrane-bound receptors. *Elife* **5**, (2016).
616 8. Sperling, M. A. *Pediatric Endocrinology-Mean Sex Steriod Concentration in Infants,*
617 *Children and adults.* (Elsevier Health Sciences, 2014).
618 9. Watts, E. L. *et al.* Prospective analyses of testosterone and sex hormone-binding globulin
619 with the risk of 19 types of cancer in men and postmenopausal women in UK Biobank. *Int J*
620 *Cancer* (2021) doi:10.1002/ijc.33555.
621 10. Barbosa-Desongles, A., Hernández, C., Simó, R. & Selva, D. M. Testosterone induces
622 cell proliferation and cell cycle gene overexpression in human visceral preadipocytes. *Am. J.*
623 *Physiol., Cell Physiol.* **305**, C355-359 (2013).
624 11. Fu, R. *et al.* Novel evidence that testosterone promotes cell proliferation and
625 differentiation via G protein-coupled receptors in the rat L6 skeletal muscle myoblast cell line. *J.*
626 *Cell. Physiol.* **227**, 98–107 (2012).
627 12. Rodríguez-Lozano, D. C., Piña-Medina, A. G., Hansberg-Pastor, V., Bello-Alvarez, C. &
628 Camacho-Arroyo, I. Testosterone Promotes Glioblastoma Cell Proliferation, Migration, and
629 Invasion Through Androgen Receptor Activation. *Front. Endocrinol.* **10**, (2019).
630 13. Maasberg, M. *et al.* Androgen receptors, androgen-dependent proliferation, and 5 alpha-
631 reductase activity of small-cell lung cancer cell lines. *Int. J. Cancer* **43**, 685–691 (1989).
632 14. Allil, P. A. A., Visconti, M. A. & Isoldi, A. M. L. C. and M. C. Photoperiod and
633 Testosterone Modulate Growth and Melanogenesis of S91 Murine Melanoma. *Medicinal*
634 *Chemistry* http://www.eurekaselect.com/82341/article (2008).
635 15. Berg, A. H., Rice, C. D., Rahman, M. S., Dong, J. & Thomas, P. Identification and
636 characterization of membrane androgen receptors in the ZIP9 zinc transporter subfamily: I.
637 Discovery in female atlantic croaker and evidence ZIP9 mediates testosterone-induced apoptosis
638 of ovarian follicle cells. *Endocrinology* **155**, 4237–4249 (2014).
639 16. Meeth, K., Wang, J. X., Micevic, G., Damsky, W. & Bosenberg, M. W. The YUMM
640 lines: a series of congenic mouse melanoma cell lines with defined genetic alterations. *Pigment*
641 *Cell Melanoma Res* **29**, 590–597 (2016).
642 17. Gao, W., Bohl, C. E. & Dalton, J. T. Chemistry and Structural Biology of Androgen
643 Receptor. *Chem Rev* **105**, 3352–3370 (2005).
644 18. Askew, E. B., Gampe, R. T., Stanley, T. B., Faggart, J. L. & Wilson, E. M. Modulation of
645 Androgen Receptor Activation Function 2 by Testosterone and Dihydrotestosterone. *J. Biol.*
646 *Chem.* **282**, 25801–25816 (2007).
647 19. Matsuura, W. *et al.* SLC39A9 (ZIP9) regulates zinc homeostasis in the secretory
648 pathway: characterization of the ZIP subfamily I protein in vertebrate cells. *Biosci. Biotechnol.*
649 *Biochem.* **73**, 1142–1148 (2009).
650 20. Fatfat, M. *et al.* Copper chelation selectively kills colon cancer cells through redox
651 cycling and generation of reactive oxygen species. *BMC Cancer* **14**, 527 (2014).
652 21. He, L. *et al.* ZIP8, member of the solute-carrier-39 (SLC39) metal-transporter family:
653 characterization of transporter properties. *Mol. Pharmacol.* **70**, 171–180 (2006).
654 22. Zhang, L. *et al.* OSskcm: an online survival analysis webserver for skin cutaneous
655 melanoma based on 1085 transcriptomic profiles. *Cancer Cell Int* **20**, 176 (2020).
656 23. Leal, M. F. *et al.* Clinical implication of 14-3-3 epsilon expression in gastric cancer.
657 *World J. Gastroenterol.* **18**, 1531–1537 (2012).
658 24. Ruas, M. & Peters, G. The p16INK4a/CDKN2A tumor suppressor and its relatives.
659 *Biochim. Biophys. Acta* **1378**, F115-177 (1998).
660 25. Germann, U. A. *et al.* Targeting the MAPK Signaling Pathway in Cancer: Promising

661 Preclinical Activity with the Novel Selective ERK1/2 Inhibitor BVD-523 (Ulixertinib). *Mol.*
662 *Cancer Ther.* **16**, 2351–2363 (2017).
663 26. Han, Y. Analysis of the role of the Hippo pathway in cancer. *Journal of Translational*
664 *Medicine* **17**, 116 (2019).
665 27. Zhao, B., Li, L., Tumaneng, K., Wang, C.-Y. & Guan, K.-L. A coordinated
666 phosphorylation by Lats and CK1 regulates YAP stability through SCFβ-TRCP. *Genes Dev* **24**,
667 72–85 (2010).
668 28. Fujii, M. Exploration of a new drug that targets YAP. *J. Biochem.* **152**, 209–211 (2012).
669 29. Bulldan, A., Malviya, V. N., Upmanyu, N., Konrad, L. & Scheiner-Bobis, G.
670 Testosterone/bicalutamide antagonism at the predicted extracellular androgen binding site of
671 ZIP9. *Biochim Biophys Acta Mol Cell Res* **1864**, 2402–2414 (2017).
672 30. Ponnusamy, S. *et al.* Orally-Bioavailable Androgen Receptor Degrader, A Potential
673 Next-Generation Therapeutic for Enzalutamide-Resistant Prostate Cancer. *Clin. Cancer Res.*
674 (2019) doi:10.1158/1078-0432.CCR-19-1458.
675 31. Chi, K. N. *et al.* Apalutamide for Metastatic, Castration-Sensitive Prostate Cancer. *N.*
676 *Engl. J. Med.* **381**, 13–24 (2019).
677 32. Kayigil, O., Atahan, O. & Metin, A. Cyproterone acetate monotherapy in advanced
678 prostatic carcinoma. *Int Urol Nephrol* **29**, 213–220 (1997).
679 33. Smalley, K. S. M. PLX-4032, a small-molecule B-Raf inhibitor for the potential
680 treatment of malignant melanoma. *Curr Opin Investig Drugs* **11**, 699–706 (2010).
681 34. Fujimura, T., Fujisawa, Y., Kambayashi, Y. & Aiba, S. Significance of BRAF Kinase
682 Inhibitors for Melanoma Treatment: From Bench to Bedside. *Cancers (Basel)* **11**, 1342 (2019).
683 35. Ørsted, D. D., Nordestgaard, B. G. & Bojesen, S. E. Plasma testosterone in the general
684 population, cancer prognosis and cancer risk: a prospective cohort study. *Ann Oncol* **25**, 712–718
685 (2014).
686 36. Bannister-Tyrrell, M., Roberts, C. L., Hasovits, C., Nippita, T. & Ford, J. B. Incidence
687 and outcomes of pregnancy-associated melanoma in New South Wales 1994–2008. *Australian*
688 *and New Zealand Journal of Obstetrics and Gynaecology* **55**, 116–122 (2015).
689 37. Gandini, S. *et al.* Hormonal and reproductive factors in relation to melanoma in women:
690 Current review and meta-analysis. *European Journal of Cancer* **47**, 2607–2617 (2011).
691 38. Testosterone - an overview | ScienceDirect Topics.
692 https://www.sciencedirect.com/topics/medicine-and-dentistry/testosterone.
693 39. Basualto-Alarcón, C., Jorquera, G., Altamirano, F., Jaimovich, E. & Estrada, M.
694 Testosterone Signals through mTOR and Androgen Receptor to Induce Muscle Hypertrophy.
695 *Medicine & Science in Sports & Exercise* **45**, 1712–1720 (2013).
696 40. Rodríguez-Lozano, D. C., Piña-Medina, A. G., Hansberg-Pastor, V., Bello-Alvarez, C. &
697 Camacho-Arroyo, I. Testosterone Promotes Glioblastoma Cell Proliferation, Migration, and
698 Invasion Through Androgen Receptor Activation. *Front. Endocrinol.* **10**, (2019).
699 41. Bulldan, A., Bartsch, J.-W., Konrad, L. & Scheiner-Bobis, G. ZIP9 but not the androgen
700 receptor mediates testosterone-induced migratory activity of metastatic prostate cancer cells.
701 *Biochim Biophys Acta Mol Cell Res* **1865**, 1857–1868 (2018).
702 42. Fukada, T. & Kambe, T. Molecular and genetic features of zinc transporters in
703 physiology and pathogenesis. *Metallomics* **3**, 662–674 (2011).
704 43. Costello, L. C., Liu, Y., Zou, J. & Franklin, R. B. Evidence for a zinc uptake transporter
705 in human prostate cancer cells which is regulated by prolactin and testosterone. *J Biol Chem* **274**,
706 17499–17504 (1999).

707 44. Bafaro, E., Liu, Y., Xu, Y. & Dempski, R. E. The emerging role of zinc transporters in
708 cellular homeostasis and cancer. *Signal Transduction and Targeted Therapy* **2**, 1–12 (2017).
709 45. Klein, S. L. & Flanagan, K. L. Sex differences in immune responses. *Nat. Rev. Immunol.*
710 **16**, 626–638 (2016).
711 46. Ma, M. *et al.* Sustained androgen receptor signaling is a determinant of melanoma cell
712 growth potential and tumorigenesis. *J Exp Med* **218**, (2021).
713

714 **Figure legends**

715 **Fig. 1: Biologic sex and testosterone promote proliferation of melanoma models lacking**
716 **detectable AR. A.** Tumor growth of human WM46 melanoma in male and female
717 immunodeficient SCID mice. Tumor doubling times are 16.99 and 19.95 days for males and
718 females respectively (Non-linear regression analysis/Exponential fit. See also Sup. Fig. 1 for
719 expanded statistical analysis). **B.** Cell proliferation (cell number) determined after 6 days of
720 treatment with vehicle (DMSO), 100nM testosterone (T) or 100nM dihydrotestosterone (DHT).
721 Human primary melanocytes (H.Mel.) and human melanoma WM46 cells are shown. Graphs
722 represent the average of three independent experiments. **C.** Cell proliferation of human WM46
723 and murine YUMM1.7 melanoma cells exposed to increasing concentrations of testosterone (T)
724 (left panels) or dihydrotestosterone (DHT) (right panel). **D.** AR protein expression determined by
725 Western blot with two different antibodies. Upper line = Androgen Receptor [(D6F11) XP®
726 Rabbit mAb #5153. Lower line = Recombinant Anti-Androgen Receptor antibody [EPR1535(2)]
727 (ab133273). The prostate cancer cell line DU 145 was used as a postivie control.). β-actin was
728 used as loading control. A replicate with increased exposure time is shown in Fig. S1G. **E.**
729 RNA-seq data from 6 different primary melanocyte cell lines reported as median FPKM (number
730 Fragments Per Kilobase of exon per Million reads). Melanocytic Receptor 1 (MC1R) and
731 Glucocorticoid Receptor (NR3C1) were used as positive controls for membrane and nuclear
732 receptors respectively.

733 ** p value≤0.01; * p value≤0.05.

734

735 **Fig 2: ZIP9 is active in human melanoma cells, and is broadly expressed in human**
736 **melanocytic tumors. A.** ZIP9 protein expression determined by western blot in primary
737 melanocytes and a battery of human melanoma cell lines. **B.** Time-lapse *in vivo* analysis of Zn^{++}

738 influx in WM46 cells upon testosterone addition (100nM). FluoZin-3 was used as Zn^{++} reporter.
739 **C.** Intracellular levels of Zn^{++} after long-term testosterone treatment (96 hours; 100nM
740 testosterone). Zinc levels were measured as fluorescence intensity per cell. FluoZin-3 was used
741 as Zn^{++} reporter. Representative images are shown on the right at indicated time-points. **D.**
742 WM46 relative proliferation (cell number) after 6 days in the presence of 100 nM testosterone
743 (T) +/- 200 nM zinc chelator (TPEN). **E.** WM46 proliferation in the presence exogenous divalent
744 cations Zn^{++} Fe^{++} and Mn^{++}. Cells were grown for 6 days and treated as indicated in the legend.
745 Error bars represent standard error of the mean (SEM). **F.** Validation of ZIP9 [(SLC39A9
746 Antibody (PA5-52485)] and androgen receptor [(Leica AR-318-L-CE, clone AR27 (clone AR27,
747 1:25)] antibodies for immunohistochemistry. ZIP9 staining performed in wild-type and ZIP9
748 knock-out cells. Non permeabilization of the cells ensured ZIP9 membrane localization. Prostate
749 gland tissue and human prostate cancer samples were used as positive controls for AR.
750 Representative images of human melanoma samples stained for ZIP9 and AR. Tumors
751 expressing low, medium and high levels of ZIP9 are shown. Replicates from the same samples
752 stained for AR are shown. 20X magnification (1.6X zoom). Scale bar=60μM. **G.** Graphic
753 representation of the % of tumors that express ZIP9. Data from nevus, primary melanomas and
754 metastatic melanoma are displayed. **H.** Graphic representation of the percentage of nevi, primary
755 lesions and metastatic tumors classified according to ZIP9 intensity (Score 1=1-25%, 2=26-50%,
756 3=51-75%, 4=76-100%).
757 **** p value≤0.0001; ** p value≤0.01; * p value≤0.05; n.s>0.05.
758
759 **Fig. 3: ZIP9 mediates testosterone effects in melanoma. A.** Proliferation (cell number) of
760 isogenic clonal populations of WM46 wtZIP9 and ΔZIP9 (gRNA #3) cells exposed to increasing
761 concentrations of testosterone (T) and dihydrotestosterone (DHT). **B.** Proliferation (cell number)

762 of isogenic clonal populations of WM46 wtZIP9 and ΔZIP9 (gRNA #4) cells exposed to
763 increasing concentrations of testosterone (T) and dihydrotestosterone (DHT). The graph
764 represents the average of three independent experiments. **C.** Intracellular levels of zinc in human
765 melanoma ΔZIP9 cells measured as relative fluorescence intensity of FluoZin-3. Graphs
766 represent the average of three independent experiments. **D.** Relative cell proliferation in the
767 presence of 100nM testosterone (T), zinc chelator (200nM TPEN) and $ZnCl_2$ (400nM). Cells
768 were cultured for 6 days. The graph represents the average of three independent experiments.
769 **** p value≤0.0001; ** p value≤0.01; * p value≤0.05; n.s>0.05.
770
771 **Fig. 4: Testosterone driven increase in melanoma proliferation requires ZIP9 and**
772 **activation of MAPK and YAP1. A.** RPPA analysis displaying changes in protein expression in
773 WM46 human melanoma cells following exposure to 100 nM testosterone (T) for increasing
774 amounts of time. Down-regulated proteins are shown in black; white color corresponds to up-
775 regulated proteins and control proteins showing no fold-change when compared to vehicle-
776 treated cells are shown in dark grey. **B.** Relative proliferation (cell number) after exposure to
777 pharmacologic ERK1/2 inhibition via 50nM RVD-523 (Ei) alone or in combination with
778 testosterone. wtZIP9 and ΔZIP9 WM46 cells are shown. The western blot shows levels of
779 phosphorylation of the ERK target RSK in wtZIP9 and ΔZIP9 WM46 cells (Ei represents RVD-
780 523). **C.** Western blot for YAP1 in fractionated WM46 lysates. Cells were treated with 100 nM
781 testosterone for the indicated times. β-Actin is used as cytoplasmic fraction positive control.
782 PARP is used as nuclear fraction positive control. Quantification of protein levels normalized
783 against T_0 is shown in the histograms (lower panel) **D.** Quantification of YAP-1 nuclear
784 immunodetection after 30 minutes of exposure to 100 nM testosterone (T) and/or 8μM

785 dobutamine (Dob) in wtZIP9 and ΔZIP9 cells. **E.** Proliferation of wtZIP9 and ΔZIP9 WM46
786 cells after treatment with 100nM testosterone (T) and/or the YAP inhibitor dobutamine (Dob). **F.**
787 Relative mRNA expression of YAP1 target genes after 30 minutes in the presence of 100 nM
788 testosterone and/or 8μM dobutamine. Error bars represent standard error of the mean (SEM).
789 *** p value≤0.001; ** p value≤0.01; * p value≤0.05; n.s>0.05.
790
791 **Fig. 5: Pharmacologic ZIP9 blockade inhibits melanoma *in vivo*. A.** Proliferation of human
792 melanoma cells (WM46) in the presence of 100 nM testosterone (T) +/- 2 μM AR inhibitors
793 (BIC:Bicalutamide; ENZ:Enzalutamide; APA:Apalutamide). Western blot showing ERK and p-
794 ERK proteins in WM46 cells treated with 100nM testosterone +/- 2μM BIC +/- 200 nM zinc
795 chelator (TPEN). **B.** Cell proliferation in human and murine derived melanoma cells [SK-MEL-3
796 (male), SK-MEL-2 (female) and YUMM1.7(male)] treated with 100 nM testosterone (T) in
797 combination with apalutamide (2 μM) (APA). **C.** Cell membrane labeling with cell impermeable
798 testosterone-BSA conjugated with FITC (0.25 μM). BSA-FITC (0.25 μM) was used as a
799 negative control for unspecific binding. Quantification of membrane labeling with T-BSA or the
800 control BSA. The graph represents the fluorescence intensity relative to the total area of each
801 cell. **D.** Proliferation of WM46 wtZIP9 and ΔZIP9 treated with 100 nM testosterone (T) in
802 combination with apalutamide (2 μM) (APA). **E.** Tumor growth and survival analysis in SCID
803 male mice bearing WM46 derived subcutaneous tumors (APA treatment: 20 mg/kg/day via oral
804 gavage). ** p-value<0.005 by ANOVA. Doubling time (non-linear regression analysis):
805 Vehicle=11.11 days; APA=25.22 days. **F.** Tumor growth in mice bearing WM46 derived
806 subcutaneous tumors. Daily treatment with bicalutamide (30 mg/kg/day, via oral gavage) or
807 vehicle are shown for both male and female mice. Linear regression analysis of slopes

808 demonstrates significant differences between vehicle treated and Bic treated males (p-
809 value<0.0001) (See Fig. S6B and S6C). **G.** Tumor growth in SCID male mice bearing ΔZIP9
810 WM46 melanoma. Mice were treated daily with bicalutamide (30 mg/kg/day) or vehicle via oral
811 gavage. . See also Sup. Fig. 6 for expanded statistical analysis).
812 **** p value≤0.0001; *** p value≤0.001; ** p value≤0.01; * p value≤0.05; n.s>0.05.
813
814 **Fig. 6: Working model.** ZIP9 activation promotes ERK phosphorylation and induces YAP1
815 nuclear translocation. AR inhibitors [represented in the figure by apalutamide (APA)] block
816 testosterone effects through ZIP9 inactivation.
817

Figure 1

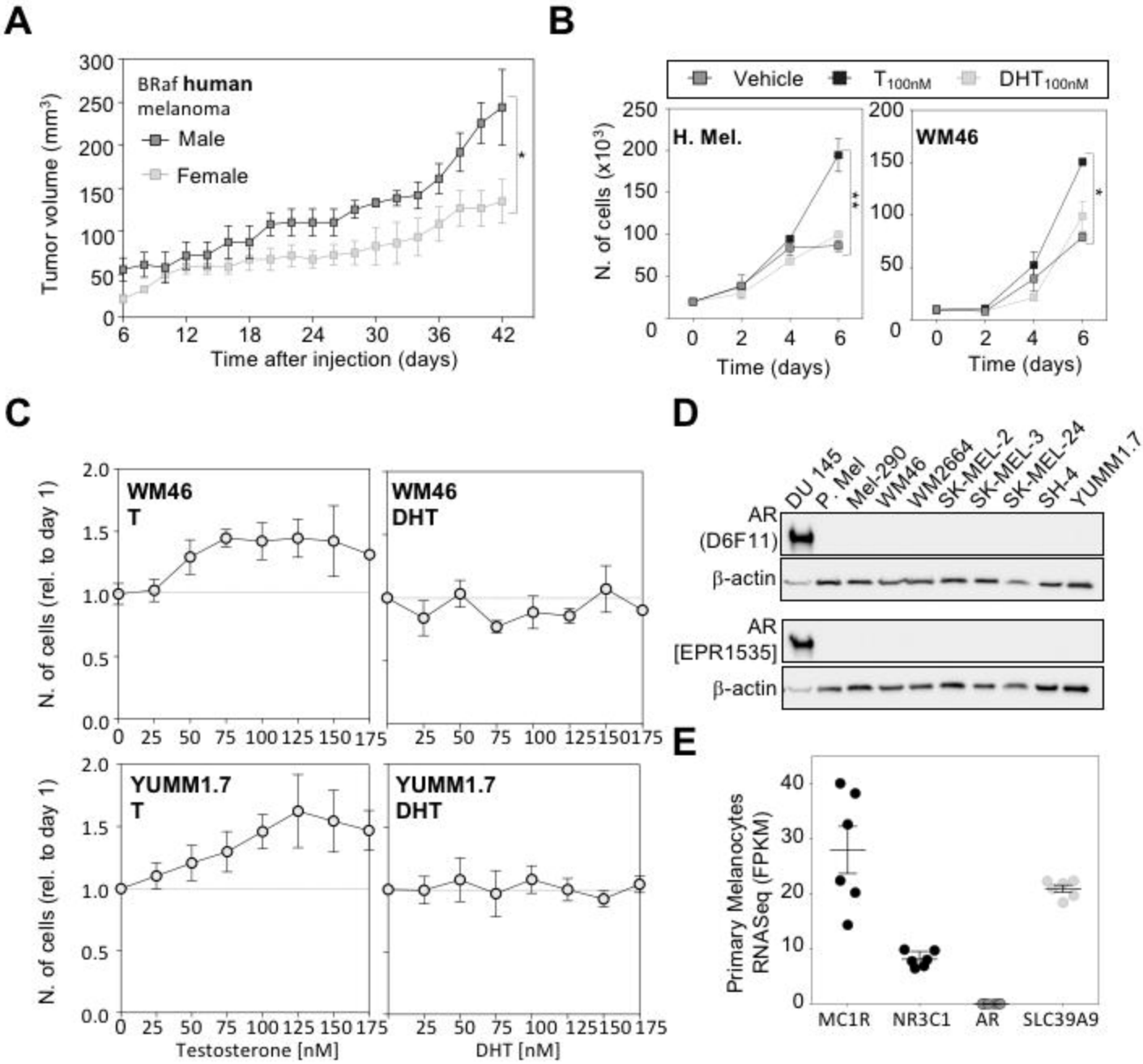
A
BRaf human melanoma
Male
Female
Tumor volume (mm³)
Time after injection (days)
B
Vehicle
T100nM
DHT100nM
H. Mel.
WM46
N. of cells (x10³)
Time (days)
C
WM46 T
WM46 DHT
YUMM1.7 T
YUMM1.7 DHT
N. of cells (rel. to day 1)
Testosterone [nM]
DHT [nM]
D
DU 145
P. Mel
Mel-290
WM46
WM2664
SK-MEL-2
SK-MEL-3
SK-MEL-24
SH-4
YUMM1.7
AR (D6F11)
β-actin
AR [EPR1535]
β-actin
E
Primary Melanocytes RNASeq (FPKM)
MC1R
NR3C1
AR
SLC39A9

Figure 2

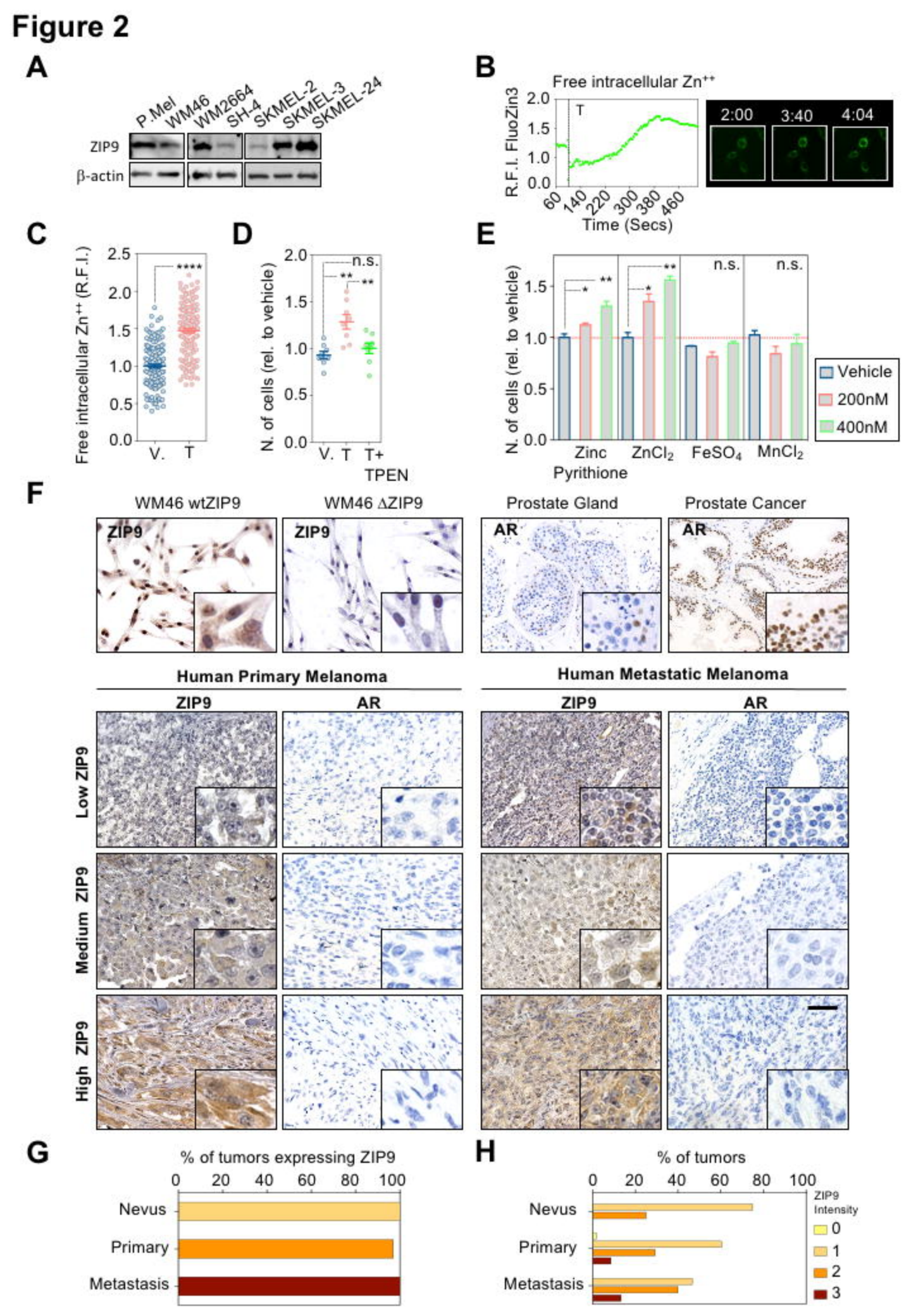
A
P.Mel
WM46
WM2664
SH-4
SKMEL-2
SKMEL-3
SKMEL-24
ZIP9
β-actin
B
Free intracellular Zn++
R.F.I. FluoZin3
T
Time (Secs)
2:00
3:40
4:04
C
Free intracellular Zn++ (R.F.I.)
****
V.
T
D
N. of cells (rel. to vehicle)
n.s.
**
V.
T
T+ TPEN
E
N. of cells (rel. to vehicle)
Zinc Pyrithione
ZnCl2
FeSO4
MnCl2
Vehicle
200nM
400nM
F
WM46 wtZIP9
WM46 ΔZIP9
Prostate Gland
Prostate Cancer
ZIP9
AR
Human Primary Melanoma
Human Metastatic Melanoma
Low ZIP9
Medium ZIP9
High ZIP9
G
% of tumors expressing ZIP9
Nevus
Primary
Metastasis
H
% of tumors
ZIP9 Intensity
0
1
2
3

Figure 3

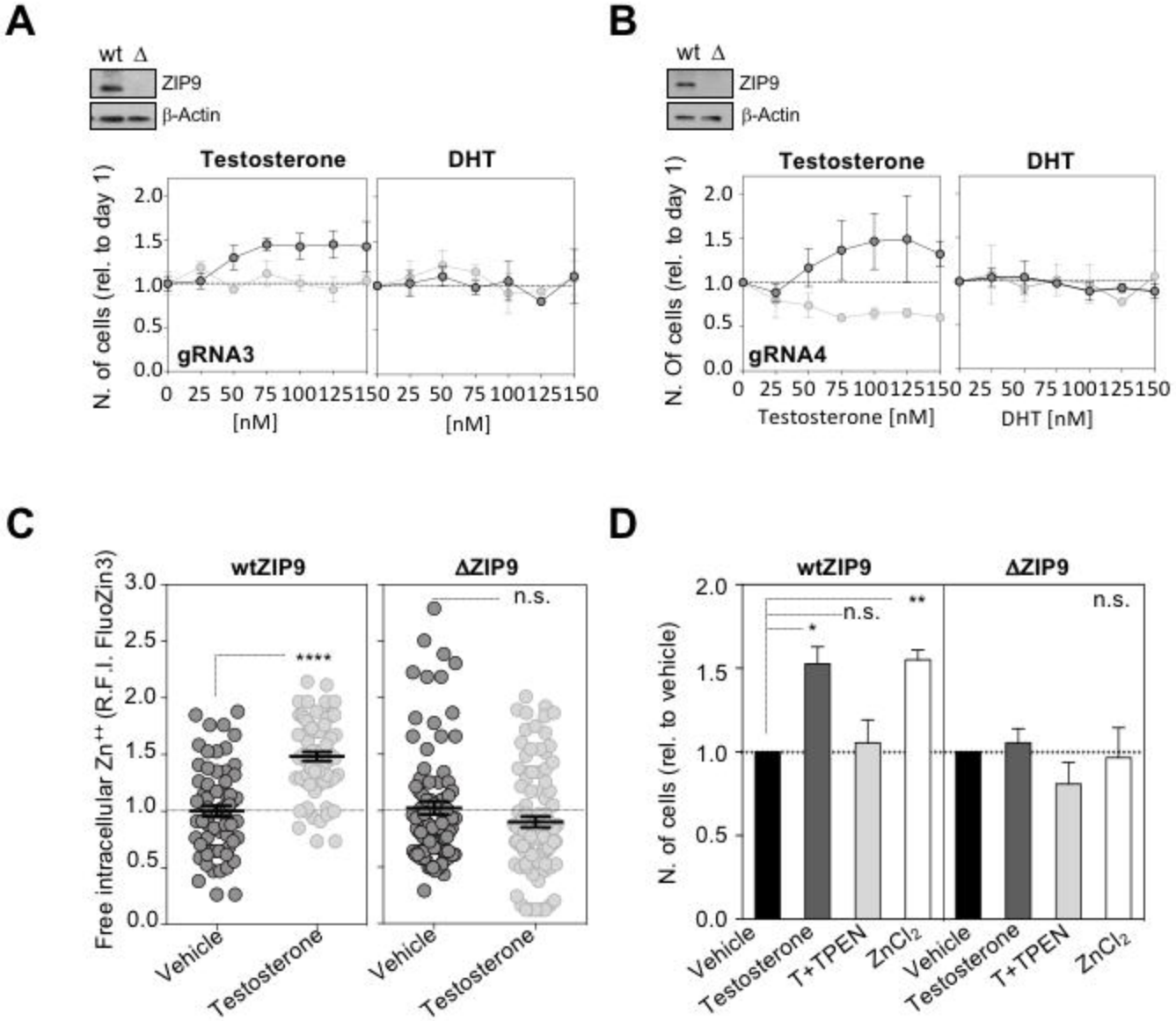
A
wt Δ
ZIP9
β-Actin
Testosterone
DHT
N. of cells (rel. to day 1)
gRNA3
[nM]
B
wt Δ
ZIP9
β-Actin
Testosterone
DHT
N. Of cells (rel. to day 1)
gRNA4
Testosterone [nM]
DHT [nM]
C
wtZIP9
ΔZIP9
Free intracellular Zn++ (R.F.I. FluoZin3)
****
n.s.
Vehicle
Testosterone
D
wtZIP9
ΔZIP9
N. of cells (rel. to vehicle)
n.s.
*
**
Vehicle
Testosterone
T+TPEN
ZnCl2

Figure 4

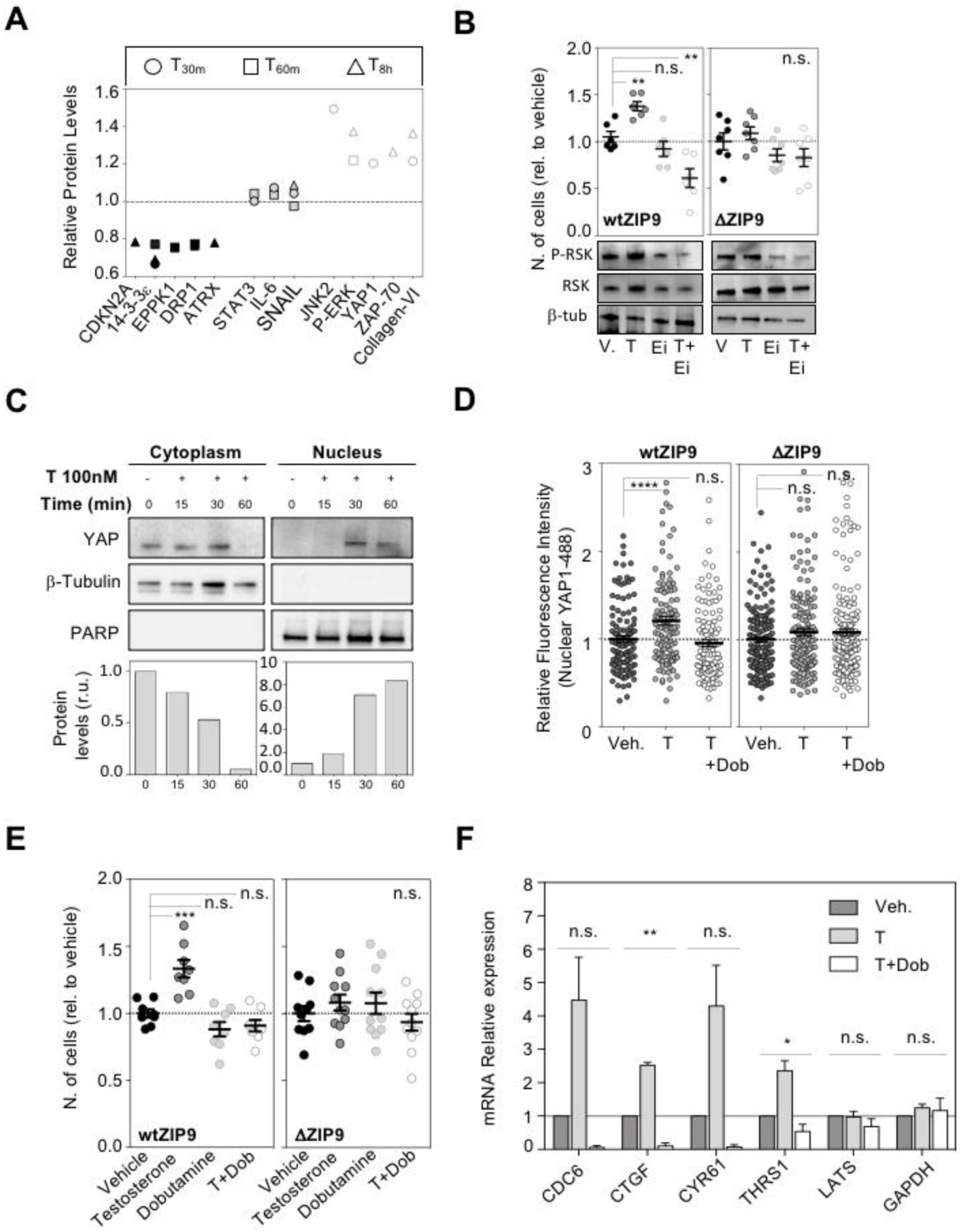
A
T30m
T60m
T8h
Relative Protein Levels
CDKN2A
14-3-3ε
EPPK1
DRP1
ATRX
STAT3
IL-6
SNAIL
JNK2
P-ERK
YAP1
ZAP-70
Collagen-VI
B
N. of cells (rel. to vehicle)
n.s.
**
wtZIP9
ΔZIP9
P-RSK
RSK
β-tub
V. T Ei T+ Ei
V T Ei T+ Ei
C
Cytoplasm
Nucleus
T 100nM
Time (min)
YAP
β-Tubulin
PARP
Protein levels (r.u.)
D
wtZIP9
ΔZIP9
Relative Fluorescence Intensity (Nuclear YAP1-488)
****
n.s.
Veh. T T +Dob
E
N. of cells (rel. to vehicle)
***
Vehicle
Testosterone
Dobutamine
T+Dob
F
mRNA Relative expression
Veh.
T
T+Dob
**
*
CDC6
CTGF
CYR61
THRS1
LATS
GAPDH

Figure 5

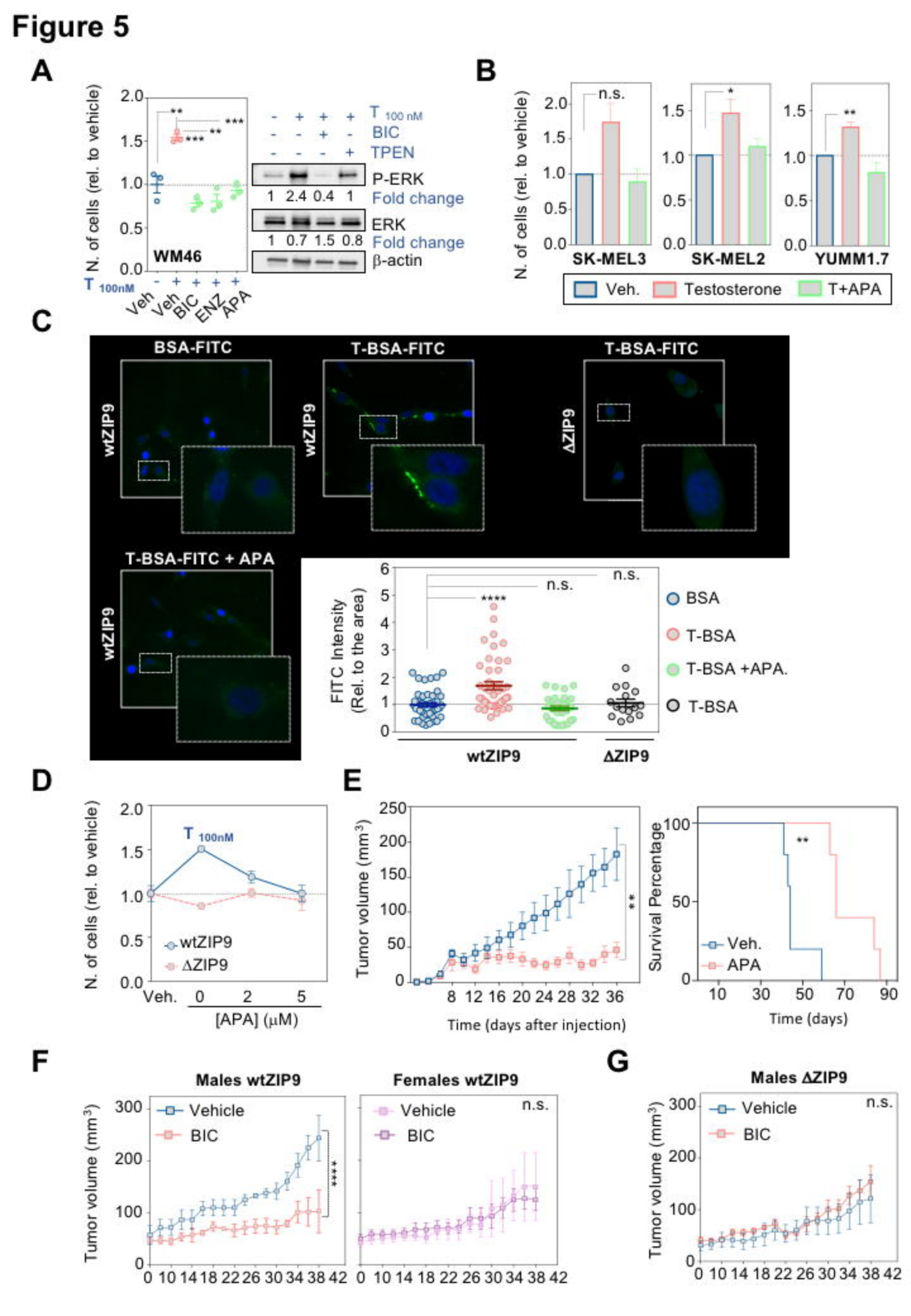
A
N. of cells (rel. to vehicle)
WM46
T 100nM
Veh
Veh
BIC
ENZ
APA
T 100 nM
BIC
TPEN
P-ERK
Fold change
1 2.4 0.4 1
ERK
Fold change
1 0.7 1.5 0.8
β-actin
B
N. of cells (rel. to vehicle)
n.s.
SK-MEL3
SK-MEL2
YUMM1.7
Veh.
Testosterone
T+APA
C
BSA-FITC
T-BSA-FITC
T-BSA-FITC
T-BSA-FITC + APA
wtZIP9
ΔZIP9
FITC Intensity (Rel. to the area)
n.s.
BSA
T-BSA
T-BSA +APA.
T-BSA
wtZIP9
ΔZIP9
D
N. of cells (rel. to vehicle)
T 100nM
wtZIP9
ΔZIP9
Veh.
[APA] (μM)
E
Tumor volume (mm³)
Time (days after injection)
Survival Percentage
Veh.
APA
Time (days)
F
Males wtZIP9
Females wtZIP9
Vehicle
BIC
n.s.
Tumor volume (mm³)
G
Males ΔZIP9
Vehicle
BIC
n.s.
Tumor volume (mm³)

Figure 6

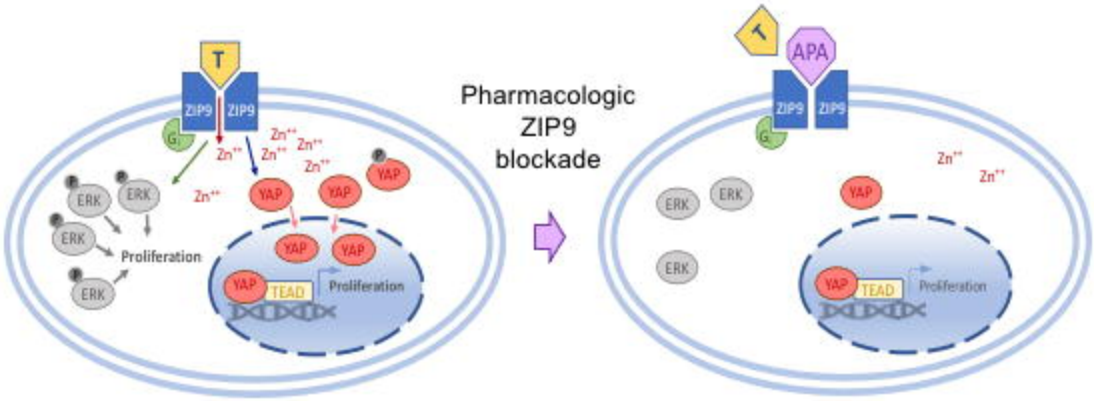
T
ZIP9
ZIP9
G
Zn++
ERK
YAP
Proliferation
TEAD
Pharmacologic
ZIP9
blockade
APA